International Journal of Technology and Applied Science (IJTAS)

E-ISSN: 2230-9004 ● Website: www.ijtas.com ● Email: editor@ijtas.com

Cyclic Strain, Tunnelling Resistance and Hysteresis in Flexible PE/PANI-Coated MWCNT Films

Dr. Jyoti Mishra

Assistant Professor
Department of Physics
D.B.S. College, Govind Nagar, Kanpur, U.P

Abstract:
Flexible films of polyethylene (PE) filled with multi-walled carbon nanotubes (MWCNTs) change their electrical resistance when stretched, and the change on unloading is rarely the same as on loading. This paper compares published data on PE/MWCNT composites, on polyaniline (PANI) coated MWCNTs and on MWCNT networks in other soft matrices. It reads them through Simmons' tunnelling picture and a tunnelling-percolation account of why the gauge factor rises with strain. The PANI shell is treated as a change in the tunnelling barrier between neighbouring tubes, not as a new conduction path. Reported gauge factors for PE matrices run from 0.6 in the elastic region of laser-sintered UHMWPE to 7.6 in printed HDPE structures, and reach 248 for an ethylene-octene copolymer with end-to-end tube contacts; silicone-based networks show resistive hysteresis of 35 to 60 percent. Direct studies of PE with PANI-coated MWCNTs under cyclic strain are scarce. We split hysteresis into lagging gap recovery in the network, viscoelastic and plastic response of the matrix, and measurement artefacts, then ask how strain rate and PE grade change the loop and why the first cycles are discarded.

Keywords: polyethylene, polyaniline-coated carbon nanotubes, tunnelling resistance, piezoresistivity, cyclic strain, electrical hysteresis

1. Introduction

Fill a polymer with enough carbon nanotubes and it conducts. How well it conducts depends on how far apart neighbouring tubes sit. Stretch the film and the tubes move apart by fractions of a nanometre, enough to change the tunnelling current across the gaps by a large factor. That is the basis of the piezoresistive composite strain sensor, and the reason it can beat a metal foil gauge on sensitivity [1].

Polyethylene is an attractive matrix for such a sensor. It is cheap, inert and melt-processable, and it comes in grades from soft LDPE to tough UHMWPE. But it is also semicrystalline with a low glass transition, so it creeps, relaxes stress and softens after a first stretch. A network pulled apart on loading does not return to the same geometry at the same strain on unloading. The resistance traces a loop, and over many cycles R0 drifts.

Coating the MWCNTs with polyaniline (PANI) by in situ polymerisation of aniline on the tube surface gives a core-shell filler. In its doped emeraldine salt form PANI conducts, so the shell is not an insulator

in the way a bare PE interlayer is; it is, though, far less conductive than the graphitic wall. It sits in the tunnelling path, where it changes the barrier height and the gap (and, through the coating step, the dispersion too).

The aim here is narrow. Given what is known about tunnelling in MWCNT networks, about PE as a viscoelastic matrix and about PANI shells, what should a PE/PANI-MWCNT film do under cyclic tensile strain, and how much of its hysteresis is electrical rather than mechanical or artefact? Everything below comes from the literature. No new measurements are reported.

2. Scientific Background and Related Research

Above the percolation threshold, current in a nanotube composite crosses two kinds of junction. Where tubes touch, the contact resistance is low. Where a thin polymer layer separates them, electrons tunnel, and the junction resistance rises exponentially with the layer thickness. Simmons derived the current density for a thin insulating film between similar electrodes [2]. Sheng later showed that thermal voltage fluctuations across small gaps set the temperature dependence of tunnelling in disordered materials [3], and Kirkpatrick's percolation treatment gives the conductivity of a random resistor network from the fraction of bonds that survive [16].

Hu and co-workers built a three-dimensional numerical model of a MWCNT/epoxy network in which the nonlinear part of the curve came from tunnelling junctions, not the tubes [4]. A later review by the same group listed where piezoresistivity comes from: tubes lose contact, tunnelling distances change, and the tubes themselves are piezoresistive [5]. Park, Kim and Youngblood measured MWCNT films in poly(ethylene oxide) at 0.56 and 1.44 vol% and saw a linear and a nonlinear region, with the shape set by how far the loading sat above the threshold [6].

Qu et al. separated the geometric part of the resistance change from the material part; in carbon black filled PDMS the conductivity fell about three orders of magnitude at 40 percent strain, which dwarfs the geometric factor of 0.96 [7]. Faeghifard et al. made sandwich-structured CNT sensors in PDMS and in thermoplastic polyurethane (TPU) over a series of CNT loadings. In cyclic tests the TPU sensors showed shoulder peaks while the PDMS ones responded at once, and the authors put this down to the mechanical hysteresis of TPU [17].

Work on polyethylene matrices is thinner. Do et al. embedded MWCNTs in UHMWPE for a knee-implant stress sensor and found a percolation threshold of 0.34 wt% [8]. Azam, Schiffer and Kumar laser-sintered MWCNT/UHMWPE [9], AlMahri et al. printed MWCNT/HDPE auxetic lattices [10], and Al Sawafi tested melt-mixed HDPE at 0.1 to 1.0 wt% [11]. None used PANI-coated tubes. The only PANI/MWCNT core-shell cyclic data we could verify are for a PANI matrix [12]. PE/PANI-MWCNT under cyclic strain has not been reported with numbers we can cite.

3. Physical Mechanisms and Analytical Approach

The resistance of a single tunnelling junction between two tubes separated by a polymer layer of thickness d follows, in the low-bias limit of the Simmons formula [2],

R_t = R_a exp(2 kappa d), with kappa = sqrt(2 m phi) / hbar.

Here R_t is the tunnelling resistance, R_a is a prefactor that depends on the junction area and on phi, m is the electron mass, hbar is the reduced Planck constant, and phi is the height of the potential barrier presented by the interlayer. For a barrier of about 1 eV, kappa is roughly 5 per nanometre, so widening d

by 0.1 nm raises R_t by a factor of about 2.7. That one number explains the sensitivity and the nonlinearity.

A picture helps. Think of the nanotubes as stepping stones, with the current hopping from stone to stone. Where stones touch, the step costs nothing. Where a thin film separates them, each extra fraction of a nanometre makes the hop far harder. Stretch the film and the stones drift apart; some hops become expensive and a few impossible.

Under a uniaxial tensile strain epsilon the gap of a junction aligned with the loading axis grows as d = d0 (1 + epsilon) in the affine picture, where d0 is the unstrained gap. The network resistance R rises with it, softened by oblique junctions and parallel routes. The usual figure of merit is the gauge factor,

GF = (delta R / R0) / epsilon,

where R0 is the resistance at zero strain and delta R = R - R0 is the change at strain epsilon. A metal foil has GF of about 2; a tunnelling network can reach tens or hundreds [1, 5].

Where do such values come from? If we take d0 = 1 nm and phi = 1 eV, then 2 kappa d0 is about 10. A strain of 1 percent stretches the aligned gap by 0.01 nm and raises R_t by about 10 percent, so a chain of such junctions gives GF near 10. Halve the barrier to 0.5 eV and GF drops to near 7; double the initial gap and the exponent doubles. GF scales with kappa d0, so the barrier and any gap set by a coating both count.

Along any current path the resistance is a series sum of the tubes' own resistance, the contact resistance where tubes touch, and the tunnelling resistance across gaps. The first is small and hardly changes with strain. Near the threshold the few spanning paths cross many gaps, so tunnelling controls R and the response is steep [4, 6]. Well above it, direct contacts carry the current, and R changes as contacts break, which gives a flatter curve [8].

Why does the curve bend upward at larger strain? Each surviving gap widens and R_t grows exponentially. At the same time, gaps that pass a cutoff distance (beyond which tunnelling is negligible) stop conducting, so the count of working junctions falls and the network drifts back toward its threshold. A tunnelling-percolation model holds both effects. Write the network conductivity as sigma proportional to (p - p_c)^t, where p is the fraction of junctions still conducting, p_c the threshold and t the conductivity exponent [16], and let p fall with strain while each surviving junction's resistance rises. At small strain the first effect gives a roughly linear delta R/R0; at larger strain the second takes over and the curve turns sharply upward as p nears p_c, the shape Park et al. measured [6] and Hu et al. simulated [4]. GF is therefore not a constant. Its local slope rises with strain, and a single-number GF describes only the range it was measured over. Azam et al.'s jump from 0.6 to 2.6 across yield [9] is this bend seen through the matrix.

The PANI shell enters through phi and d0. A bare PE interlayer is a wide-gap insulator with a high barrier. Doped PANI has a much lower one, so kappa is smaller and the same gap change gives a smaller fractional rise in R_t. The shell also adds thickness to every junction, raising d0 and R0. We would expect a higher baseline and a gentler, more linear curve. Whether it also reduces hysteresis depends on whether the glassy PANI cracks or debonds during cycling.

Electrical hysteresis is defined here as the difference between the resistance on unloading and on loading at the same strain, normalised to the full-scale change:

H = (R_unload(epsilon) - R_load(epsilon)) / (R_max - R0).

Mechanical hysteresis is the matching loop in the stress-strain curve, and the two need not coincide. A junction that opened on loading may close only after the matrix has relaxed, so R lags strain even when

stress does not; this is the intrinsic electrical part. Stress relaxation, creep and Mullins-type softening (a lower stress on the second stretch than on the first) belong to the matrix, and they shift R0 between cycles. Electrode slip, strain rate and temperature form a third layer. The affine picture assumed a constant barrier and a fixed junction count; both fail under exactly these conditions.

Strain rate ties the loop width to a time scale. Suppose the amorphous fraction of the PE relaxes with a characteristic time tau after a step in strain. If the cycle period T is long compared with tau, the network settles at every point and the loop is narrow. If T is comparable to tau, the unloading branch sits well above the loading branch, because gaps opened on the way up have not closed on the way down. Mu et al. saw the time dependence in silicone as a relaxation ratio (the share of the resistance step that decays while strain is held) that rose with amplitude from 10 to 30 percent and fell with loading [14]. Lin et al. loaded their PANI/MWCNT sample at only 0.00254 cm/min and still saw a step in the load-time curve [12]. The ratio tau/T belongs next to H in any report; a loop measured at one rate says little about another.

4. Results from the Literature and Scientific Discussion

A gauge factor of 0.6 in the elastic region and 2.6 once the material yields: that is what Azam et al. measured in laser-sintered MWCNT/UHMWPE, and their hexagonal lattices held a linear response with GF of 1 over 100 cycles [9]. Below yield the crystalline lamellae carry the load and the tube gaps barely move. Above it the amorphous fraction flows and irreversibility grows. Crystallinity also decides where the tubes sit. Growing lamellae push nanotubes out into the amorphous layers between them, and Azam et al. found that 0.5 wt% MWCNT raised the crystallinity of their UHMWPE by about 10 percent [9]. So the network ends up in the softest fraction of the solid, which takes most of the strain and recovers slowly (one reason a semicrystalline matrix can show electrical hysteresis while its mechanical loop stays narrow). Do et al., in compression, saw a cyclic coefficient of variation below 5 percent. Their 0.3 wt% samples were more sensitive than the 0.5 wt% ones but less linear, which they attributed to changes in tunnelling resistance within the network [8]; that fits a 0.5 wt% network sitting further above the 0.34 wt% threshold. AlMahri et al. reached GF of 7.6 in a printed HDPE auxetic lattice at 4 wt% MWCNT by letting the cell geometry amplify the local strain [10].

Pu et al.'s ethylene-octene block copolymer is a polyethylene relative with a soft elastomeric phase. By arranging MWCNTs in end-to-end contact networks they got a gauge factor of 248 at 5 percent strain, with a linear response and stretching to 300 percent [13]. Bundled tubes slide before they disconnect. End-to-end contacts do not. The loop width is not reported.

Table 1. Reported strain response and cyclic behaviour of MWCNT networks in polyethylene-type and reference matrices.

Ref.	Matrix and filler	Strain amplitude and loading	Cycles	GF or delta R/R0	Hysteresis or recovery	Explanation given
[9]	UHMWPE, MWCNT (0.5 wt% raised	Tension, elastic and inelastic	100	GF 0.6 elastic, 2.6 inelastic;	Consistent and stable sensing over 100	Uniform dispersion, low porosity

	crystallinity by about 10 percent), laser sintered	regimes		lattice GF 1	cycles	(about 1 percent)
[10]	HDPE, 4 wt% MWCNT, printed auxetic lattice	Tension	not read	GF 7.6 (S-shaped cell)	not reported in abstract	Cell geometry amplifies local strain; empirical sensitivity vs relative density
[8]	UHMWPE, 0.3 and 0.5 wt% MWCNT	Quasi-static and short cyclic compression	short cyclic test	Resistance falls with stress; higher coefficient at 0.3 wt%	Repeatable, coefficient of variation below 5 percent	Change in tunnelling resistance within the network
[13]	Ethylene-octene block copolymer, MWCNT in 2D end-to-end network	Tension to 300 percent	cycling durability reported	GF 248 at 5 percent strain, linear	High cycling durability	End-to-end contacts disconnect without a sliding phase
[12]	PANI matrix, 11 wt% PANI-coated MWCNT	Quasi-static load to about 0.0006 strain	6 load/unload cycles	Slope changes in three strain regions; no single GF	Did not return to zero after unloading; drift of -0.1298 mV/h	Partly machine unloading profile; step in load-time curve shrank with cycles
[14]	Silicone rubber, 0.5 to 3 wt% CNT and 2 to 6 wt% CB	10, 20 and 30 percent tension	cyclic	GF 18.6 (0.5 wt% CNT), 22.3 (3 wt% CB)	Resistive hysteresis lowest at 59.6 percent (3 wt% CNT) and 35.0 percent (6 wt% CB); relaxation ratio rises with strain	Network change near threshold at low loading; unrecoverable deformation at high loading
[15	SBS,	Dynamic	repeated	Highest	Melt-mixed:	Disordered,

]	MWCNT, melt vs solution mixed	uniaxial strain	cycles	sensitivity near percolation	drift and shoulder peaks; solution-mixed: reversible each cycle	loosely packed melt-mixed network breaks more easily

The stiff semicrystalline matrices show the smallest hysteresis, at the price of a gauge factor near unity, while soft matrices with high GF carry loops a third to two thirds of full scale [14]. Mu et al. give the clearest split. Near the threshold the hysteresis comes from the network, since opened junctions re-form slowly and not always in the same place; at high loading it comes from unrecoverable deformation of the filler-rich matrix [14]. A 0.5 wt% UHMWPE composite sits close to its 0.34 wt% threshold [8], so the network term should dominate there until the strain passes yield.

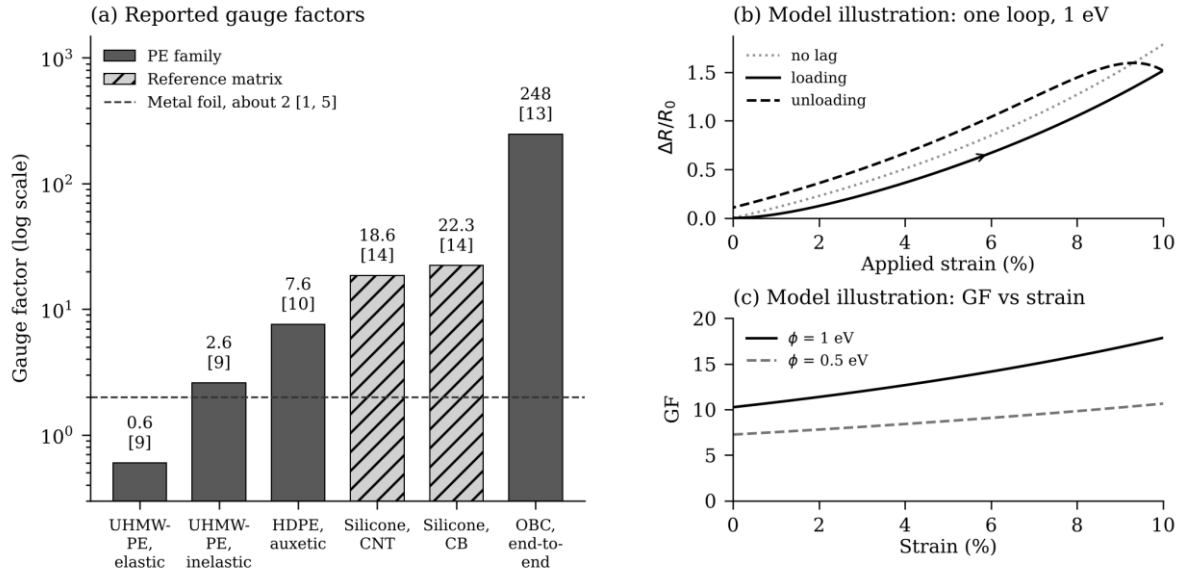


Figure 1. (a) Gauge factors reported in the sources of Table 1 and the text, on a log scale: laser-sintered MWCNT/UHMWPE below and above yield [9], a printed MWCNT/HDPE auxetic lattice [10], silicone rubber with 0.5 wt% CNT and with 3 wt% CB [14], and an ethylene-octene block copolymer (OBC) with end-to-end MWCNT networks at 5 percent strain [13]. Dark bars are PE-family matrices, hatched bars are reference matrices, and the dashed line marks the gauge factor of about 2 for a metal foil [1, 5]. (b) and (c) Model illustrations, not measured data. Both use a single aligned junction in the affine picture of Section 3, delta R/R0 = exp(2 kappa d0 epsilon) - 1, with d0 = 1 nm and kappa = sqrt(2 m phi)/hbar, and ignore oblique junctions, rerouting and loss of junctions. In (b), phi = 1 eV and the applied strain rises linearly from 0 to 10 percent and returns to 0 over one period T. The gap is assumed to follow the applied strain with a first-order lag, d epsilon_g/dt = (epsilon - epsilon_g)/tau, starting from rest, with tau/T = 0.05 chosen only for illustration; the dotted curve is the no-lag limit. In (c), GF = (delta R/R0)/epsilon for phi = 1 eV and 0.5 eV.

The bars in panel (a) span a factor of about 400. Why? Panel (c) gives a yardstick: one aligned 1 nm junction starts at GF = 2 kappa d0, about 10 at 1 eV and 7 at 0.5 eV, and reaches only about 18 at 10 percent strain. The silicone composites, at 18.6 and 22.3, sit close to that scale. The PE values below yield sit well under it. That shortfall is the stiff matrix shielding the network. If 2 kappa d0 is near 10, a GF of 0.6 means the gaps stretch by about 6 percent of the applied strain (a model inference, not a measurement). The HDPE lattice reaches 7.6 through geometry [10]. And 248 at 5 percent strain is more than ten times what one affine junction gives there (about 13 at 1 eV); no plausible barrier closes that gap. The extra factor is network geometry. End-to-end contacts let go together, so the count of conducting junctions falls toward the threshold [13, 16] instead of each gap widening a little.
Panel (b) shows a purely electrical lag. Unloading lies above loading, the order Mu et al. report in silicone [14], and at zero strain delta R/R0 is still about 0.1, decaying at the rate set by tau. Even with tau/T = 0.05 the loop is about a fifth of full scale at mid-strain. How would one tell this from matrix creep? Hold the film at zero strain after the cycle. An intrinsic network lag relaxes back toward R0, and narrows when the cycle is slowed. Creep or plastic set in the matrix leaves an offset that survives the hold, shows up as residual strain in the stress-strain loop, and adds up from cycle to cycle. A no-lag curve fitted to a slow loading branch gives an effective 2 kappa d0, and a loop that survives very slow rates with no stress residual means junctions re-form in new places rather than late. The two terms need not even move together: in Mu et al.'s silicone, mechanical hysteresis rose with loading while resistive hysteresis did not [14].

Filler loading changes more than the gauge factor. In Mu et al.'s silicone, GF fell with filler content from 18.6 at 0.5 wt% CNT, and resistive hysteresis first fell as loading rose above the threshold and then rose again, with minima of 59.6 percent for 3 wt% CNT and 35.0 percent for 6 wt% CB [14]. So a composite just above threshold pays for its high GF with a wide loop and hold-time drift, and adding filler trades sensitivity for stability only until the matrix yields. Do et al.'s UHMWPE shows the same trade [8].
The first cycle is rarely like the rest. Lin et al. saw a step in their load-time curve that shrank with each of six cycles [12]. Mu et al. found more hysteresis in the first loading cycle than in later ones, and report that low-loading CNT composites lost sensitivity over repeated cycling while CB ones held up better [14]. Duan et al.'s melt-mixed SBS drifted and grew shoulder peaks under dynamic strain; their solution-mixed samples, with a more tightly packed network, did not [15]. But shoulder peaks can also come from the matrix: Faeghifard et al. saw them in TPU and not in PDMS [17]. Most of this is shakedown. On the first stretch the weakest junctions (the loosely bundled or poorly wetted ones) break and do not re-form, and what remains survives the working amplitude with a narrower loop and a lower but steadier GF. Shakedown measures how much of the as-made network was never going to last. Since PE is almost always melt-processed, a PE/PANI-MWCNT film may need more of it than a solution-cast elastomer, unless the shell improves dispersion.

Over six quasi-static cycles Lin et al.'s PANI-matrix sensor did not return to zero after unloading, though a foil gauge tested alongside it did [12]. They put part of the residual down to the machine's unloading profile, a warning that artefacts can pass for material hysteresis. Their drift of -0.1298 mV/h, against -0.0866 mV/h for the foil gauge, was measured at constant strain. It is a relaxation of the network or shell, not a strain effect.

What, then, should a PE/PANI-MWCNT film do under cyclic tensile strain? From Section 3 and the matrix data we expect a lower GF than for bare MWCNTs in the same PE, because the shell lowers phi and raises d0, and a response closer to linear over a wider range. The shell should also shrink the network term of the hysteresis, since tubes wrapped in PANI are less likely to form the overlapped bundles that Pu et al. link to sliding [13]. The matrix term is set by the PE grade. These are extrapolations.

HDPE is highly crystalline and stiff, while LDPE, with its branched chains, is far less crystalline and much softer. Below yield, the amorphous layers that hold the tubes in HDPE see only a fraction of the applied strain. We would expect a low GF, a narrow loop and little drift, much as Azam et al. found for UHMWPE [9]. LDPE is different. Its amorphous fraction is larger and its yield strain higher, so the same applied strain reaches more of the network; GF should be higher and the loop wider, and creep and Mullins softening in the softer matrix should shift R0 more between cycles. LLDPE sits between the two. HDPE and UHMWPE suit a stable small-strain sensor, LDPE suits sensitivity at the cost of calibration effort, and the PANI shell changes the barrier in all of them without changing this order.

Two further effects of the coating are hypotheses, not findings. PANI is itself piezoresistive. A strained shell changes its own conductivity, and if it carries part of the junction current its response adds to, or subtracts from, the tunnelling signal (the sign for a shell wrapped round a tube is not known). PANI is also sensitive to humidity, since water uptake changes its doping state, so a film in open air could show a slow R0 drift unrelated to strain and a loop whose width follows the weather. Neither has been measured in this system.

5. Practical Implications and Limitations

For a flexible strain sensor on PE, the data argue for working below yield and well above the percolation threshold. That gives up sensitivity (GF near 1 rather than tens) but buys a loop narrow enough to calibrate with one curve, and it keeps R0 drift within reach of re-zeroing [8, 9]. For large strain an elastomeric ethylene copolymer with a designed network is the better route [13].

What else would a working PE sensor need? A strain range that stops at yield, with the calibration fitted over that range only. A single slope where the response is linear enough, and a stored lookup curve where it is not. Temperature compensation, because R0 moves with thermal expansion and with the fluctuation-induced term in tunnelling [3]; the usual answer is an unstrained element of the same film in a half-bridge, so that both arms drift together and only strain survives. And encapsulation, since PE is a good moisture barrier but the electrodes, cut edges and any PANI shell are not.

Electrodes are the artefact most often mistaken for material behaviour. A painted or clamped contact on a PE film has its own resistance. It changes with strain as the paint cracks or the clamp relaxes, with a lag of its own, so it adds a loop that looks like hysteresis in the composite. Lin et al. traced part of their residual to the test machine [12], and a contact can do the same. Two checks are cheap. A four-wire measurement, with current fed through outer contacts and voltage read between inner ones, takes the contact resistance out of the reading. Measuring the loop at two electrode spacings on the same strip separates the sources: a loop that scales with gauge length belongs to the film, and one that does not belongs to the contacts. A strain rate fast against the matrix relaxation time inflates the loop (Section 3). Heat speeds relaxation and narrows the loop but raises R0 through expansion. A fixed strain rate and a

thermostat deal with both. The shakedown data [12, 14] suggest one more habit: condition the film with cycles at or above the working amplitude, discard them, and calibrate on the loop that remains.

The main limitation is the lack of direct PE/PANI-MWCNT cyclic data. The expectations in Section 4 rest on a tunnelling model whose barrier parameters for a PANI shell are not known precisely, and on matrix behaviour taken from bare-tube PE. The shell may also crack or dedope with repeated stretching, raising phi over the cycles and adding its own drift. Several sources report compressive or quasi-static loading rather than tensile cycling. And the HDPE versus LDPE comparison above is reasoned, not measured.

6. Conclusion

In a flexible polymer, a MWCNT network sets its resistance through tunnelling gaps that respond exponentially to strain. That is why the gauge factor climbs with strain and why the loop between loading and unloading records how slowly those gaps close compared with the matrix. Stiff semicrystalline PE gives gauge factors of order one and cycles stably; soft elastomer networks are more sensitive but carry loops a third to two thirds of full scale. Strain rate, PE grade and the electrode contacts can each add a loop of their own, and each can be checked. A PANI shell should lower the barrier and flatten the curve at the cost of a higher baseline, though its piezoresistance and its response to humidity are still unmeasured. Nobody has yet put coated and bare MWCNTs into the same PE and compared the loops. That is the experiment this comparison asks for.

REFERENCES:

[1] M. Amjadi, K.-U. Kyung, I. Park, and M. Sitti, "Stretchable, skin-mountable, and wearable strain sensors and their potential applications: A review," Adv. Funct. Mater., vol. 26, no. 11, pp. 1678-1698, 2016, doi: 10.1002/adfm.201504755.

[2] J. G. Simmons, "Generalized formula for the electric tunnel effect between similar electrodes separated by a thin insulating film," J. Appl. Phys., vol. 34, no. 6, pp. 1793-1803, 1963, doi: 10.1063/1.1702682.

[3] P. Sheng, "Fluctuation-induced tunneling conduction in disordered materials," Phys. Rev. B, vol. 21, no. 6, pp. 2180-2195, 1980, doi: 10.1103/PhysRevB.21.2180.

[4] N. Hu, Y. Karube, C. Yan, Z. Masuda, and H. Fukunaga, "Tunneling effect in a polymer/carbon nanotube nanocomposite strain sensor," Acta Mater., vol. 56, no. 13, pp. 2929-2936, 2008, doi: 10.1016/j.actamat.2008.02.030.

[5] Alamusi, N. Hu, H. Fukunaga, S. Atobe, Y. Liu, and J. Li, "Piezoresistive strain sensors made from carbon nanotubes based polymer nanocomposites," Sensors, vol. 11, no. 11, pp. 10691-10723, 2011, doi: 10.3390/s111110691.

[6] M. Park, H. Kim, and J. P. Youngblood, "Strain-dependent electrical resistance of multi-walled carbon nanotube/polymer composite films," Nanotechnology, vol. 19, no. 5, art. 055705, 2008, doi: 10.1088/0957-4484/19/05/055705.

[7] M. Qu, Z. Xie, S. Liu, J. Zhang, S. Peng, Z. Li, C. Lin, and F. Nilsson, "Electric resistance of elastic strain sensors: Fundamental mechanisms and experimental validation," Nanomaterials, vol. 13, no. 12, art. 1813, 2023, doi: 10.3390/nano13121813.

[8] Q. Do, S. O'Byrne, M. Liu, and L. Zhang, "Piezoresistive behavior of MWCNT-UHMWPE composite for compressive stress sensing applications," IEEE Trans. Nanotechnol., vol. 16, no. 2, pp. 265-273, 2017, doi: 10.1109/TNANO.2017.2662087.
[9] M. U. Azam, A. Schiffer, and S. Kumar, "Mechanical and piezoresistive behavior of selectively laser sintered MWCNT/UHMWPE nanocomposites," Compos. Part A Appl. Sci. Manuf., vol. 173, art. 107701, 2023, doi: 10.1016/j.compositesa.2023.107701.
[10] S. AlMahri, J. Schneider, A. Schiffer, and S. Kumar, "Piezoresistive sensing performance of multifunctional MWCNT/HDPE auxetic structures enabled by additive manufacturing," Polym. Test., vol. 114, art. 107687, 2022, doi: 10.1016/j.polymertesting.2022.107687.
[11] S. Al Sawafi, "Polymer/carbon nanotube nanocomposites for strain sensing applications," Latv. J. Phys. Tech. Sci., vol. 62, no. 2, pp. 81-90, 2025, doi: 10.2478/lpts-2025-0015.
[12] W. Lin, Y. Rotenberg, K. P. Ward, H. Fekrmandi, and C. Levy, "Polyaniline/multi-walled carbon nanotube composites for structural vibration damping and strain sensing," J. Mater. Res., vol. 32, no. 1, pp. 73-83, 2017, doi: 10.1557/jmr.2016.361.
[13] J.-H. Pu, X.-J. Zha, L.-S. Zhao, S. Li, R.-Y. Bao, Z.-Y. Liu, B.-H. Xie, M.-B. Yang, Z. Guo, and W. Yang, "2D end-to-end carbon nanotube conductive networks in polymer nanocomposites: a conceptual design to dramatically enhance the sensitivities of strain sensors," Nanoscale, vol. 10, no. 5, pp. 2191-2198, 2018, doi: 10.1039/c7nr08077h.
[14] Q. Mu, T. Hu, X. Tian, T. Li, and X. Kuang, "The effect of filler dimensionality and content on resistive viscoelasticity of conductive polymer composites for soft strain sensors," Polymers, vol. 15, no. 16, art. 3379, 2023, doi: 10.3390/polym15163379.
[15] L. Duan, S. Fu, H. Deng, Q. Zhang, K. Wang, F. Chen, and Q. Fu, "The resistivity-strain behavior of conductive polymer composites: stability and sensitivity," J. Mater. Chem. A, vol. 2, no. 40, pp. 17085-17098, 2014, doi: 10.1039/c4ta03645j.
[16] S. Kirkpatrick, "Percolation and conduction," Rev. Mod. Phys., vol. 45, no. 4, pp. 574-588, 1973, doi: 10.1103/RevModPhys.45.574.
[17] P. Faeghifard, M. Mehranpour, and I. Ghasemi, "Fabrication and investigation on mechanical, electrical, and sensing performance of polydimethylsiloxane/carbon nanotube and thermoplastic polyurethane/carbon nanotube wearable strain sensors," Adv. Eng. Mater., vol. 27, no. 7, art. 2402208, 2025, doi: 10.1002/adem.202402208.